Desalination and Water Treatment
www.deswater.com

doi: 10.5004/dwt.2018.21936

103 (2018) 102–112
January

Adsorption of cationic dye from aqueous solution using molecularly imprinted polymers (MIPs)

M.A. Zulfikar[a,*], Mustapa[a], M.B. Amran[a], A. Alni[b], D. Wahyuningrum[b]

[a]*Analytical Chemistry Research Group, Institut Teknologi Bandung, Jl. Ganesa 10, Bandung 40132, Indonesia, email: zulfikar@chem.itb.ac.id (M.A. Zulfikar), mustchemist@gmail.com (Mustapa), amran@chem.itb.ac.id (M.B. Amran)*
[b]*Organic Chemistry Research Group, Institut Teknologi Bandung, Jl. Ganesa 10, Bandung 40132, Indonesia, email: alni@chem.itb.ac.id (A. Alni), deana@chem.itb.ac.id (D. Wahyuningrum)*

Received 7 March 2017; Accepted 25 January 2018

ABSTRACT

In this study, molecularly imprinted polymers (MIPs) were prepared using the microwave-assisted organic synthesis method for the adsorption of methylene blue (MB), a cationic dye, from aqueous solutions. The preparation of dye-MIP was carried using methacrylic acid (MAA) as monomers, divinyl benzene (DVB) as a cross-linker and acetonitrile as a porogen. The control polymer materials, i.e. the NIPs, were also prepared in a similar way to that of the MIPs preparation, but without the MB molecule as a template. The characterization of both the obtained NIPs and dye-MIPs was achieved by FTIR, SEM and Brunauer-Emmett-Teller (BET) method. Finally, both the obtained NIPs and dye-MIPs were used for the adsorption of MB from aqueous solutions using the batch adsorption technique. The effects of various experimental parameters, such as contact time, pH, adsorbent dosages, initial MB concentration and temperature on the adsorption capacity were investigated. The results showed that the adsorption behavior of both NIPs and dye-MIPs was greatly affected by the pH and initial concentration of MB. The experimental data were also analyzed by the Langmuir and Freundlich models of adsorption. The adsorption of MB onto both NIPs and dye-MIPs is in accordance with the Langmuir isotherm models with the adsorption capacity, which was found to be 33.11 and 40.82 mg/g, respectively. Thermodynamic parameter data indicated that the MB adsorption process onto dye-MIPs was non spontaneous and exothermic under the experimental conditions, with the values of Gibbs free energy (ΔG^o) being in the range of 1.02 to 3.76 kJ mol^{-1}; as well as the values of enthalpy (ΔH^o) and entropy (ΔS^o) that were found to be –19.35 kJ mol^{-1} and –68.39 J mol^{-1}, respectively. Moreover, pseudo-first-order, pseudo-second-order, intra-particle-diffusion, and Boyd kinetic models were considered to evaluate the rate parameters. The adsorption process could be described well by a pseudo-second-order model.

Keywords: Adsorption; Cationic dye; Kinetics; Methylene blue; Molecularly imprinted

1. Introduction

Water contamination caused by dye industries, including food, leather, textiles, plastics, cosmetics, paper-making, printing and dye synthesis, has caused increasing attention, since most dyes are harmful to humans beings and environments [1]. Some dyes and their degradation products have carcinogens and toxic properties, so the removal of dyes from wastewater becomes an important issue in the environmental protection. Moreover, dyes in wastewater can obstruct light penetration and have a high visibility; hence, conditions are not good for the life of the water [2].

Methylene blue belongs to one of the primary classes of commercial dyes, and is stable in the visible and near-UV ranges of light [3]. Methylene blue (MB) ($C_{16}H_{18}N_3SCl$) as a thiazine cationic dye is commonly used to color paper, temporary hair colorants, dyeing of cotton, wood, and silk [3–6]. Although MB is not considered to be a very toxic dye, it can cause some harmful effects such as vomiting, increased heart rate, diarrhea, shock, cyanosis, jaundice,

*Corresponding author.

quadriplegia, and tissue necrosis on human beings [5–8]. Consequently, MB containing wastewater should be treated before discharge.

Physical adsorption using solid adsorbents has been a promising method for treating dyes, pigments and other colorant wastewater, owing to its advantages such as operational simplicity, low cost, availability in large amount and ability to treat pollutants in a sufficiently large-scale operation [9,10]. One of the most widely used adsorbents in the wastewater treatment industry is activated carbon because of its large specific surface area property in spite of it being a bit expensive to be used in such systems [11,12]. Moreover, the use of activated carbon also has several limitations, such as high cost associated with its production and regeneration, has a lower reusability, and it is only limited to the removal of non-polar materials [10,13,14]. Therefore, there is a need to find the effective materials for dyes wastewater treatment.

Molecularly imprinted polymers (MIPs) are the type of synthesized materials with specific recognition capability for the template of the substrate molecules. In comparison with the absorbents commonly used, the MIPs have a higher reusability and selectivity, economic and environmental-friendly, and lower consumption [15,16]. In recent reports, MIPs have been widely used in many fields, such as solid-phase extraction [17,18], chromatographic separation [19], membrane separations [20,21], sensors [22,23] and biological ones [24–26]. The molecularly imprinting technique has also been applied to environmental fields [16,27–29]. The removal of MB from an aqueous solution by molecularly imprinted polymers (MIPs) as an adsorbent has been reported [30–32]. The use of an MB-MIP, prepared by bulk polymerization via radical polymerization containing MB as a template, methacrylic acid as a monomer, ethylene glycol dimethacrylate as a cross-linker, benzoyl peroxide as an initiator and tetrahydrofuran as a solvent (porogen) for the removal of MB from an aqueous media, was studied by Asman et al. [30,31]. Recently, Wang et al. [32] synthesized MB-MIPs using inverse microemulsion polymerization with MB as a template, acrylic acid as a monomer, N,N′- methylene bisacrylamide (MBA) as the cross-linking agent, 2,2′-azobis (2-methylpropionitrile) (AIBN) as the initiator, and acetonitrile as the organic solvent for adsorption of MB from water. However, as far as we know, there are no reports on the synthesis of MB-MIPs via radical polymerization using microwave-assisted organic synthesis (MAOS) method containing MB as a template, methacrylic acid as a monomer, divinyl benzene (DVB) as a cross-linker, 2,2′-azobis (2-methylpropionitrile) (AIBN) as the initiator and acetonitrile as porogen. Therefore, the main objective of this study was the synthesis of hydrophilic MB-molecularly imprinted polymers using microwave assisted organic synthesis (MAOS) method and being applied for removing water-soluble cationic dyes from wastewater. The physical properties of the MIPS were characterized by Fourier transform infra-red (FT-IR) spectroscopy, scanning electron microscope (SEM) and Brunauer-Emmett-Teller (BET) method. The adsorption of MB onto MIPs microspheres, including effects of initial solution pH, agitation time, initial concentration, adsorbent dosage and temperature, was systematically investigated by batch adsorption experiments. The Langmuir and Freundlich isotherm models were used to evaluate the equilibrium adsorption data. The kinetics of the removal process were determined using pseudo-first-order, pseudo-second-order and intra-particle-diffusion kinetic models. Besides, we also thoroughly studied the thermodynamics of the adsorption process.

2. Materials and methods

2.1. Materials

MIP that has been prepared from methacrylate acid (MAA) as a monomer, methylene blue, C.I. 52015 (MB) as templates, divinyl benzene (DVB) as a cross-linker and acetonitrile as porogen, was purchased from Merck. The hydrochloric acid used to adjust the pH was purchased from Merck. Also, the water used was generated from aqua demineralization system. All materials were used without further purification.

2.2. Synthesis of dye-MIPs

The preparation of dye-MIPs material was done by mixing 2 mmol of MAA, 10 mmol of DVB and 0.50 mmol MB as a template. This solution was then cooled to 0°C and purged with Nitrogen for 30 min. Futhermore, the prepared solution was added dropwise from a pipette into an AIBN solution (0.0466 ml) and then put in the microwave at a temperature of 65°C for 5 min followed by a temperature of 70°C for 5 min while stirring continuously. The obtained materials were grounded in a mortar and dried in a hot air oven at 60°C for 2 h, and then sieved to acquire the powdered particles. The machine was set to automatically sieve the grinded sample at a particle size in the range of 60–80 µm. About 5 g of these powdered particles were subjected to leaching with 200 ml of methanol-acetic acid mixture (9:1 v/v) for 5 h to obtain dye-MIPs materials, and then washed with methanol. After washing, the sorbent particles were dried by means of a vacuum, after which they were ready for use. The control polymer materials, i.e. the NIPs, were prepared in a similar way to that of the dye-MIPs preparation, but without the MB molecule as a template.

2.3. Characterization

FTIR spectra of dye-MIPs were obtained by means of a Perkin Elmer 3100 FTIR spectrophotometer, in the range of 4000–5000 cm^{-1} using KBr pellets containing the prepared materials. The resolution for each spectrum was 2 cm^{-1}. Scanning electron microscopy of the prepared particles was carried out using a JEM-2010JEOL scanning microscope equipped with an energy-dispersive X-ray (EDX) Oxford ISIS 300 micro-analytical system. The surface area of dye-MIPs was analyzed by nitrogen adsorption measurements at 77 K using Micromeritics Gemini 2370 (USA) equipment.

2.4. Sorption studies

Adsorption experiments were carried out by agitating 50 mg each of both dye-MIPs and NIPs with 25 ml of the dye solution of the desired concentration (100 mg/l) and

pH 10 at 150 rpm, the temperature being 25°C in a thermostated rotary shaker (ORBITEK, Chennai, India) for 10, 20, 30,60, 90, 120, 150 and 180 min. The samples were withdrawn from the shaker at predetermined time intervals and the dye solution was separated from the adsorbent by centrifugation at 20,000 rpm for 20 min. The supernatant was then analyzed for the remaining MB concentration by an ultraviolet-visible spectrophotometer model UV-Vis 1601 (Shimadzu, Japan) at 663 nm. Duplicate samples were measured, and the average will be used in subsequent analysis.

The percent of MB adsorption was calculated using the following equation:

$$\%\ Adsorption = \frac{C_i - C_e}{C_i} \times 100 \quad (1)$$

where C_i and C_e are initial and final concentration (mg/l) of MB in solution, respectively. The adsorption capacity of an adsorbent at equilibrium with solution volume V, was calculated using the following equation:

$$q_e(\mathrm{mg/g}) = \frac{C_i - C_e}{m} \times V \quad (2)$$

where C_i and C_e are the initial and final concentration (mg/l) of MB in solution, respectively. V is the volume of the solution (L) and m is mass of adsorbent (g) used.

The influence of pH on dye adsorption capacity was studied by mixing every 50 mg of both dye-MIPs and NIPs with 25 ml of an aqueous dye solution (C_o = 100 mg/l). Immediately after mixing, the suspension was allowed to adsorb the dyes by shaking at 150 rpm for 12 h (contact time). The temperature was maintained constant at 25°C using a thermostated rotary shaker (ORBITEK, Chennai, India). The pH value, ranging between 2 and 12, was kept constant throughout the entire adsorption process with micro-additions of 0.1 M HNO_3 or 0.1 M NaOH.

The effects of the adsorbent dosage on dye adsorption capacity were investigated by agitating different dosages of dye-MIPs and NIPs particles (10–150 mg) in 25 ml MB 100 mg/l for 60 min at pH of 10 and shaking speed at 150 rpm.

The effect of temperature on the dye adsorption capacity was determined by shaking 50 mg of dye-MIPs in 25 ml MB at four different temperatures of 25, 45, 65, and 80°C at pH of 10 and shaking speed at 150 rpm.

The effect of the initial dye concentration was determined by contacting 50 mg of dye-MIPs with 25 m of aqueous dye solutions (C_o = 10–100 mg/l). Immediately after mixing, the suspension was allowed to adsorb the dyes by shaking at 150 rpm for 60 min (at pH = 10, determined as optimum value) at 25°C.

The effect of cadmium and lead ions on the adsorption of MB onto dye-MIPs experiments was conducted at varying metal ion concentrations between 10 and 50 mg/l. The pH of the solutions was also set at 7 using 0.1 M HNO_3 and NaOH. In the experiments, 50 mg of dye-MIPs were added into a test solution (25 ml) containing both metals (cadmium or lead) and MB. The adsorption conditions were kept the same as described earlier.

2.5. Study of adsorption isotherms

The study of adsorption was determined by contacting each of the 50 mg of both dye-MIPs and NIPs with 25 ml of aqueous dye solutions (C_o = 10–300 mg/l). Immediately after mixing, the suspension was allowed to adsorb the dyes by shaking for 60 min (at pH = 10, determined as optimum value) at 25°C. The same experiments were repeated at 45 and 65°C.

2.6. Study of adsorption kinetics

Batch kinetic experiments were performed by mixing a fixed amount of dye-MIPs (50 mg) with 25 ml of an aqueous dye solution (60, 80 and 100 mg/l). The suspensions were shaken for 10, 20, 30,60, 90, 120, 150 and 180 min at pH = 10 (optimum adsorption pH value found from the pH-effect experiments) at 25°C. Samples were collected at fixed intervals and analyzed using a UV Vis spectrophotometer.

2.7. Desorption experiments

Desorption of the sorbed MB dyes from the imprinted polymers was studied in a batch experimental set-up. After adsorption, the samples were collected and filtered using fixed pore size membranes. Desorption experiments were performed by mixing the collected amount of loaded dye-MIPs with both HCl and HNO_3 solutions over a concentration range of 0.1–0.5 mol/l. After 24 h of shaking at 25°C, samples were taken and the analysis revealed the optimum desorption.

3. Results and discussion

3.1. Characterization of dye-MIPs and NIPs

The FT-IR spectra of the dye-MIPs before and after removing the template as well as the NIPs, all prepared under the optimal conditions, are presented in Fig. 1. It can be seen from Fig. 1 that the FTIR spectrum between NIPs,

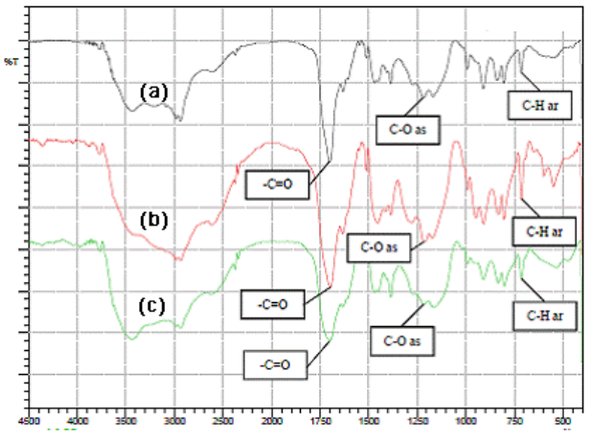

Fig. 1. FT-IR spectrum of (a) NIPs, (b) dye-MIPs before, and (c) dye-MIPs after removing the template.

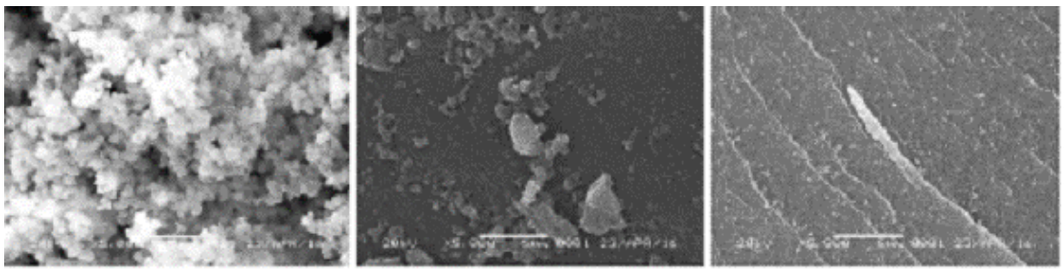

Fig. 2. Surface morphology of (a) NIPs, (b) dye-MIPs before, and (c) dye-MIPs after removing the template.

dye-MIPs before and after removing the template has a similar pattern and this shows that the polymer framework of the third structure is almost the same. The broad peak around 3440 cm^{-1} is assigned to the hydroxyl groups. The bands around 1690 cm^{-1} are assigned to the stretching vibrations of C=O, while the peaks at 1215 cm^{-1} are assigned to the stretching vibration bands of –C-OH.

Fig. 2 shows the SEM image of the NIPs, dye-MIPs before and after removing the template. High magnification SEM image shows that the surface of NIPs (Fig. 2a) is much rougher than both of dye-MIPs before and after removing the template. The surface of dye-MIPs before removing the template looks more refined than the NIPs (Fig. 2b) and a small quantity of particles appear on its surface. After removing the template, the surface of dye-MIPs (Fig. 2c) becomes smoother than before removing the template.

The surface areas of both NIPs and dye-MIPs were determined by nitrogen sorption (BET) measurements. The surface areas of both NIPs and dye-MIPs were 5.94 and 83.34 m^2/g, respectively; close to the range of imprinted polymers [24,33]. In general, polymers made in "poor" solvents tend to have a lower surface area than polymers made in "good" solvents [25,29,33]. The higher surface area presents advantages of perfect binding-site integrity, total accessibility of imprinted sites, excellent mass transport and finely adjusted hydrodynamic properties [33].

3.2. Adsorption studies

3.2.1. Effect of pH on dye adsorption

pH plays an important role in aqueous chemistry and surface binding sites of the adsorbents. As shown in Fig. 3, the adsorption capacity of MB onto both dye-MIPs and NIPs is a pH-dependent phenomenon. The adsorption capacities of MB present a significant upward trend from 16.81 to 49.28 mg/g for dye-MIPs and 6.78 to 36.22 mg/g for NIPs with the increase of pH values in the range of 2–12. It suggests that dye-MIPs microspheres can be a high-efficiency adsorbent for the adsorption of MB in basic solutions. It can be ascribed to the dissociation of functional groups on the active sites of the adsorbent, the changes in surface charge of the adsorbent and aqueous chemistry of dye molecules [1,34,35].

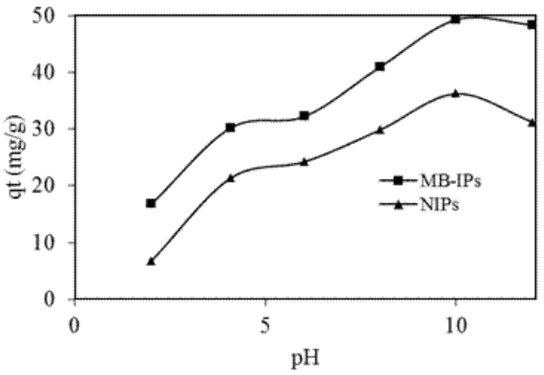

Fig. 3. The effect of pHs on MB adsorption capacity from aqueous solution (contact time: 60 min, volume 25 mL, conc. 100 mg/L, dosage 0.05 g, shaking speed 150 rpm, and temp. 25°C).

3.2.2. Effect of agitation time

Optimizing the effect of time in the adsorption system is necessary to develop cost-effective procedure. In wastewater treatment procedure, decreasing the removal time is necessary [36]. The effect of the agitation time on MB adsorption capacity by both NIPs and dye-MIPs materials are shown in Fig. 4. The results showed that, in general, the adsorption of MB using NIPs and dye-MIPs occurred in two stages; a rapid adsorption stage in the first 60 min and a slower adsorption stage at 60–180 min. Based on the figure, by continuing the process of adsorption, the adsorption sites will be gradually occupied by molecular substrate and will slowly increase the adsorption capacities of MB. After 60 min, the adsorption capacities of MB exhibited no visible changes. At the beginning of the adsorption, MB adsorption occurs by surface adsorption (external surface adsorption). At a later stage (slower adsorption stage), the adsorption occurs mainly through the transport of surface-adsorbed dye to the internal sites of the adsorbent (internal surface adsorption) [37,38].

3.2.3. Effect of inital concentration

The amount of adsorption for dye removal is highly dependent on the initial dye concentration. The effect of

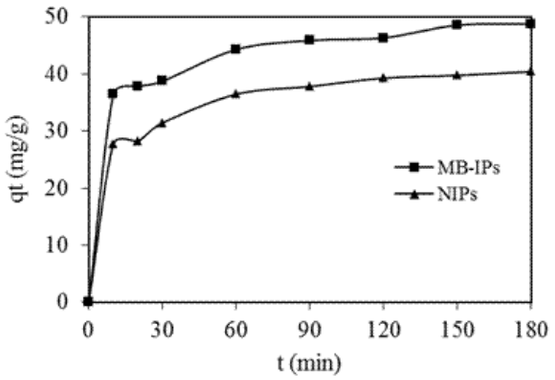

Fig. 4. The effect of agitation time on MB adsorption capacity (pH 10, volume 25 mL, conc. 100 mg/L, dosage 0.05 g, shaking speed 150 rpm, and temp. 25°C).

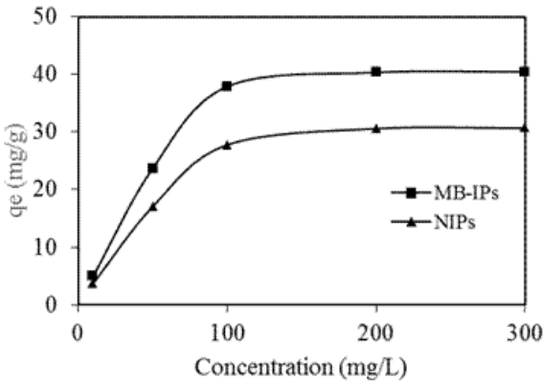

Fig. 5. The effect of initial concentration on MB adsorption capacity (pH 10, volume 25 mL, dosage 0.05 g, shaking speed 150 rpm, and temp. 25°C).

the initial dye concentration depends on the immediate relationship between the concentration of the dye and the available sites on an adsorbent surface. In general, the percentage of dye removal decreases with an increase in the initial dye concentration, which may be due to the saturation of adsorption sites on the adsorbent surface [39]. The effect of initial dye concentration on MB adsorption capacity by both NIPs and dye-MIPs materials are shown in Fig. 5. It is observed that the amount of MB dye adsorbed, (q_t), increased from 4.98 to 40.33 mg g^{-1} for dye-MIPs and 3.71 to 30.58 mg g^{-1} for NIPs as the initial dye concentration increased from 10 to 200 mg/l, respectively. This indicates that the initial dye concentration plays a significant role in the adsorption capacity of the dye. This increase in the amount of adsorption is due to the fact that in batch adsorption, the initial dye concentration provides the driving force to overcome the resistance to the mass transfer of dye between the aqueous and the solid phase. For constant dosage of adsorbent, at a higher initial dye concentration, the available adsorption sites of adsorbent become fewer, and hence the removal of MB depends on the initial concentration [39,40]. The increase in the initial concentration also enhances the interaction between the adsorbent and the dye. Therefore, an increase in the initial dye concentration leads to an increase in the adsorption uptake of dye [39].

3.2.4. Effect of dosages

The amount, size and pore volume of the adsorbent significantly influence the capacity of adsorption towards various molecules. Generally, the vacant site and pore size of the adsorbent limit the rate and amount of migration of the dye molecule to the adsorbent surface [4].

The effect of the amount of NIPs and dye-MIPs on the MB adsorption capacity was studied at different adsorbent doses and their results are shown in Fig. 6. It can be seen that the MB adsorption percentage increases with increased dosage up to 0.10 g, after which it remained fairly constant despite the increase in the amount of the dye-MIPs microsphere to 0.15 g. At equilibrium time, the % adsorption increased from 56.31 to 94.12% for

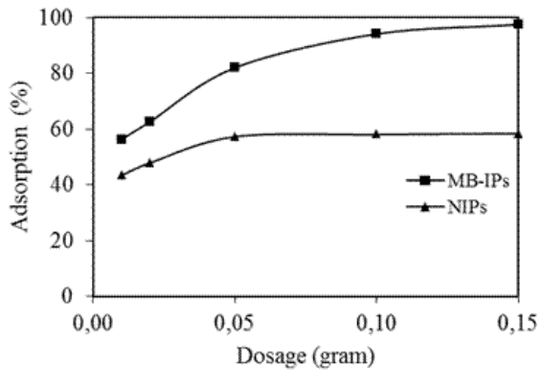

Fig. 6. The effect of dosages on MB adsorption capacity (pH 10, volume 25 mL, conc. 100 mg/L, shaking speed 150 rpm, and temp. 25°C).

an increase in dye-MIPs dose from 0.01 to 0.10 g. The increase in % adsorption was due to the increase in the available sorption surface and the availability of more adsorption sites.

3.2.5. Effect of ions

The influence of ions on the adsorption capacities of MB onto dye-MIPs was also investigated by varying the Cd^{2+} and Pb^{2+} ions concentration from 10 to 50 mg/l because the adsorption process in some cases is markedly affected by the existence of electrolytes due to their interference in the electrostatic interaction between the adsorbate and absorbent, drastically impacting the adsorption process [40–42]. However, contrary to expectations, the presence of copper and lead ions did not find significant changes in MB adsorption capacity when increasing both the Cd^{2+} and Pb^{2+} ions concentration (Fig. 7). These results suggest that the binding affinity between MIPs and dye molecules is not significantly affected by the concentrations of background ions; thus, the adsorption of MB predominantly takes place

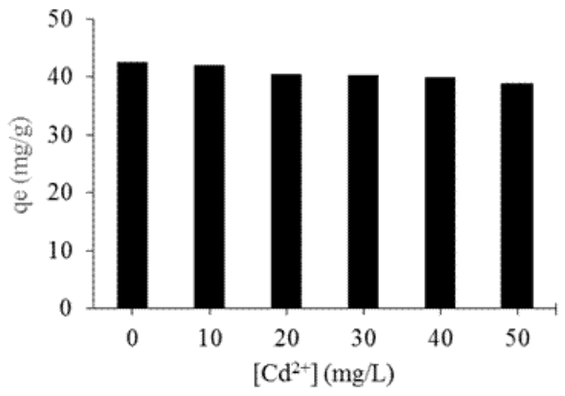

(a)

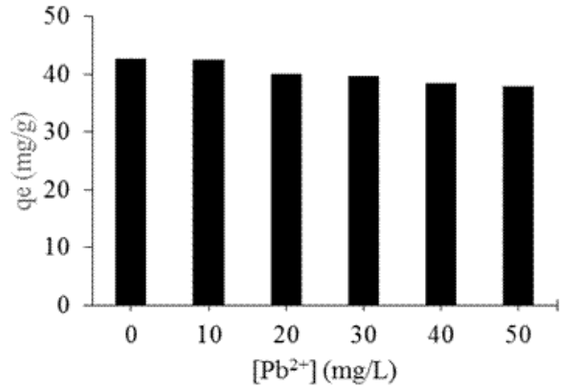

(b)

Fig. 7. The effect of ions Cd(II) (a) and Pb(II) (b) on MB adsorption capacity (pH 7, volume 25 mL, conc. 100 mg/L, shaking speed 150 rpm, and temp. 25°C).

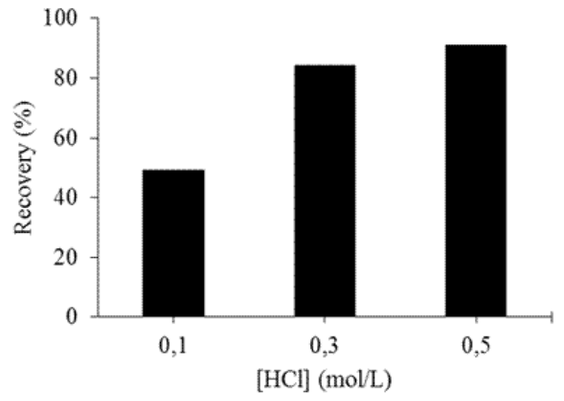

(a)

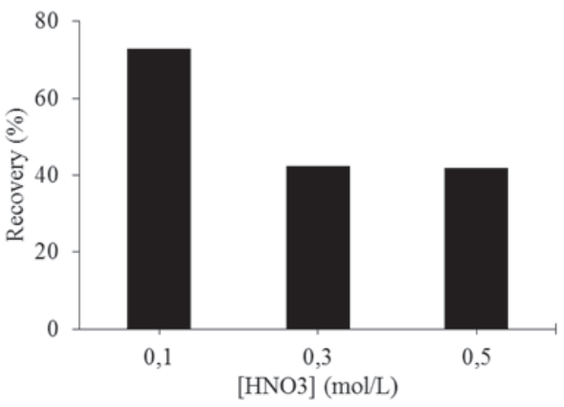

(b)

Fig. 8. Desorption study with different solutions HCl (a) and (b) HNO_3.

at the internal layer of dye-MIPs rather than the external layer because the latter could be more prone to the influence of ionic intervention than the former [43].

3.2.6. Desorption study

Desorption study is usually applied to elucidate the adsorption mechanism and to recover the depleted adsorbent [44,45]. In this study, two solutions were used: hydrochloric acid solution and nitric acid solution. To compare the efficiency of different solutions in desorption study, the concentration of solution was set at 0.1–0.5 mol/l. According to Fig. 8, hydrochloric acid solution is the most efficient compared to nitric acid solution.

3.3. Isotherms of adsorption

The adsorption equilibrium isotherm is important for describing how the adsorbate molecules are distributed between the liquid and the solid phases when the adsorption process reaches an equilibrium state. The most widely used isotherm equations are the Langmuir and Freundlich equations. Langmuir isotherm is based on the assumption that an activation point on the surface of the adsorbent is able to adsorb one molecule, indicating that the adsorbed layer has one molecule of thickness. It is expressed as:

$$q_e = \frac{q_m \cdot b \cdot C_e}{1 + b \cdot C_e} \tag{3}$$

where C_e (mg/l) is the equilibrium concentration, q_e (mg/g) is the amount adsorbed, q_m (mg/g) is the complete monolayer adsorption capacity, and b (L/mg) is the Langmuir constant. The dimensionless separation factor, R_L, is an essential characteristic of Langmuir isotherm, which is defined as:

$$R_L = 1/(1+b \cdot C_o) \tag{4}$$

where b is the Langmuir constant and C_o is the highest initial MB concentration. The value of R_L indicates the type of the isotherm to be either favorable ($0 < R_L < 1$), unfavorable ($R_L > 1$), linier ($R_L = 1$) or irreversible ($R_L = 0$) [10].

The Freundlich isotherm model is derived by assuming a heterogeneous surface of adsorption capacity and adsorption intensity with a non-uniform distribution of adsorption heat, in which it is characterized by the heterogeneity factor, $1/n$. The empirical equation can be written as:

$$q_e = K_f C_e^{1/n} \quad (5)$$

where C_e is the equilibrium concentration (mg/l), q_e is the amount of adsorbate adsorbed per unit weight of absorbent (mg/g), and K_f and n are Freundlich constants. A value of $1/n$, ranging between 0 and 1, is a measure of adsorption intensity or surface heterogeneity. A value for n greater than one indicates of a favorable adsorption process. The other Freundlich constant K_f indicates the adsorption capacity of the adsorbent.

The Langmuir and Freundlich isotherms for the system studied are presented in Fig. 9, and their parameters computed from Eqs. (4), (5) are listed in Table 1. The best fit isotherm model for the system was compared by judging the correlation coefficients, R^2 values. The higher correlation coefficient of the Langmuir isotherm than those of Freundlich (Table 1) suggests that the experimental results fit the Langmuir isotherm model best, with the adsorption capacity found to be 33.11 and 40.82 mg/g for NIPs and dye-MIPs, respectively. This finding is consistent with the conclusion obtained from the effect of the initial dye concentration on adsorption capacity.

The R_L values obtained from the Langmuir isotherm constant K_L are between 0 and 1, indicating that the MB adsorption process onto both NIPs and dye-MIPs is favorable (Table 1) [10].

3.4. Kinetics of adsorption

The kinetic of adsorption was investigated to predict the rate of dye removal from the aqueous solutions. Several kinetic models including pseudo-first-order, pseudo-second-order and intra-particle diffusion are available to understand the behaviour of the adsorbate that was successfully adsorbed onto the adsorbent surface and determines the controlling mechanism of the adsorption process. The pseudo first-order model is one of the most widely used equations to describe the adsorption rate based on the adsorption capacity. The linear form is formulated as:

$$\log (q_e - q_t) = \log q_e - (k_1/2.303)\, t \quad (6)$$

where k_1 is the adsorption rate constant (min^{-1}), q_e and q_t are the amounts of MB adsorbed at equilibrium and at time t (min). The values of k_1 and q_e (Table 2) were evaluated from the linear regression of log ($q_e - q_t$) versus t (Fig. 10a). The determination coefficient value for the pseudo-first-order adsorption model (R^2) was very high and close to unity.

The pseudo-second order model is based on the adsorption capacity of the dye molecules on the surface of the adsorbent and its linear form is expressed as follows:

$$t/qt = 1/k_2 \cdot q_e^2 + t/q_e \quad (7)$$

where k_2 (g/(mg min^{-1})) is the rate constant of pseudo-second-order adsorption. The values of k_2 and q_e (Table 2) were calculated from the slope and intercept of straight portion of the linear plots obtained by plotting t/q_t against t (Fig. 10b). After the calculation, if the adsorption data followed the pseudo-second order model, the overall rate of the dye adsorption process was controlled by the chemisorption process.

The results in Table 2 show that the coefficient of determination for the second-order kinetic model is low and the calculated equilibrium adsorption capacity q_e has a large deviation in comparison with the experimental data. It suggested that the pseudo-second-order model is not suitable

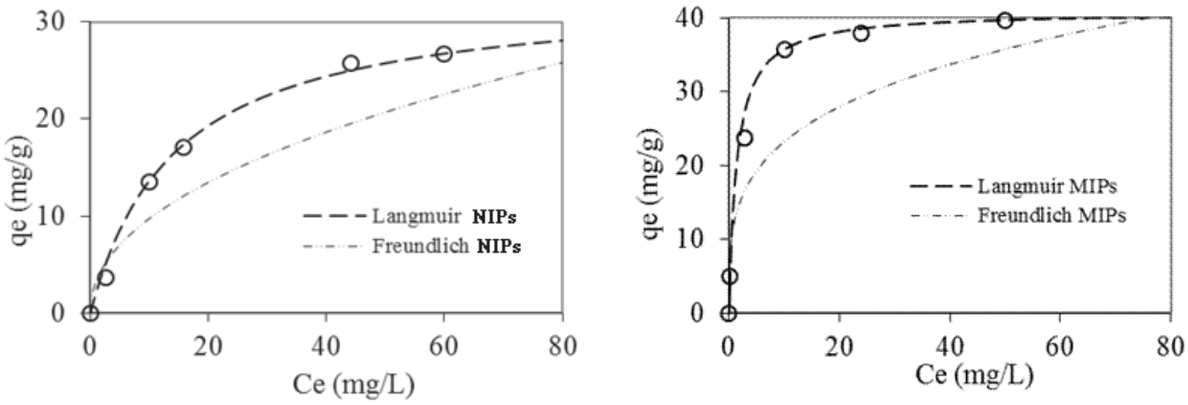

Fig. 9. Adsorption isotherms and fitting curves of NIPs and dye-MIPs towards MB with different initial concentrations.

Table 1
Langmuir and Freundlich parameters for MB adsorption onto NIPs and dye-MIPs

Adsorbents	Langmuir Model			Freundlich Model			q_{mexp} (mg/g)	R_L
	b (L/mg)	q_m (mg/g)	R^2	n	K_f (mg/g)	R^2		
NIPs	0.07	33.11	0.997	2.14	3.32	0.863	30.67	4.54×10^{-2}
dye-MIPs	0.70	40.82	0.999	3.73	12.53	0.897	40.44	4.74×10^{-3}

Table 2
Pseudo-first and pseudo second order kinetics parameters for MB adsorption onto dye-MIPs

Concentration	Pseudo-first-order			Pseudo-second-order			
(mg/L)	k_1 (min^{-1})	$q_{e,cal}$ (mg/g)	R^2	k_2 (g/(mg min^{-1}))	$q_{e,cal}$ (mg/g)	R^2	$q_{e,exp}$ (mg/g)
60	0.0214	17.62	0.847	0.0025	31.25	0.985	29.27
80	0.0184	17.85	0.909	0.0039	38.02	0.996	37.48
100	0.0223	22.41	0.818	0.0036	49.50	0.997	48.75

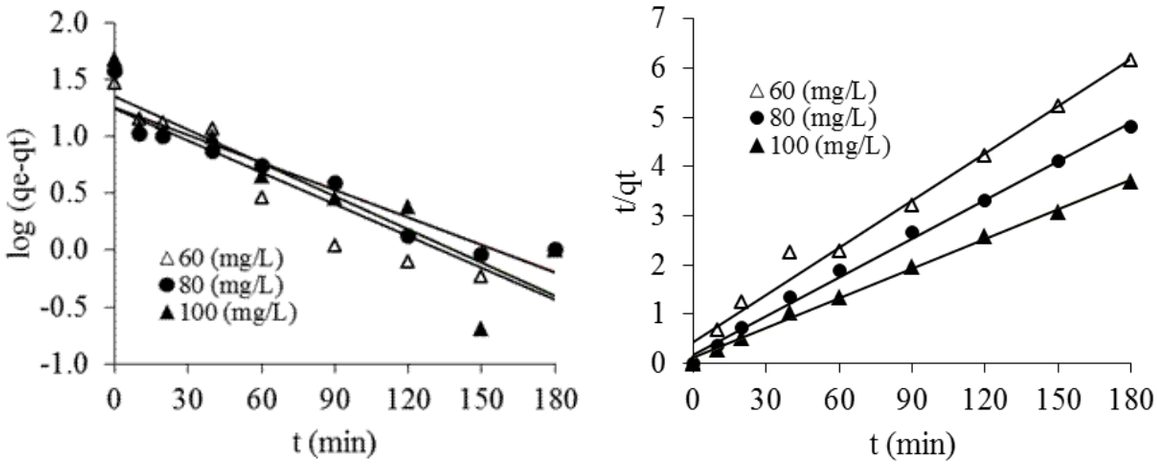

Fig. 10. Pseudo-first-order (a) and pseudo-second-order (b) models plot for MB adsorption at different concentration (volume 25 mL, dosage 0.05 g, pH 10, shaking speed 150 rpm and temp. 25°C).

to describe the adsorption of MB onto dye-MIPs and the rate-limiting step is not chemisorption.

Adsorption kinetics is usually controlled by different mechanisms, and in general is by diffusion mechanism. If the experiment is a batch system with rapid stirring, there is a possibility that the transport of sorbate from solution into pores (bulk) of the adsorbent is the rate-controlling step [46,47].

This possibility was tested in terms of a graphic relationship between the amount of dye adsorbed and the square root of time. Since the MB is probably transported from its aqueous solution to the dye-MIP by intra-particle diffusion, so the intra-particle diffusion is another kinetic model that should be used to study the rate-limiting step for MB adsorption onto dye-MIP. The intra-particular diffusion is commonly expressed by the following equation [28,48,49]:

$$q_t = k \cdot t^{1/2} + C \quad (8)$$

where k and C are an intra-particle diffusion rate constant (mg/g·min$^{1/2}$) and a constant, respectively. The k is obtained from the slope of linear plot of q_t vs. $t^{1/2}$. The values of q_t were found to give two lines part with values of $t^{1/2}$ (Fig. 11), and the rate constant k is evaluated directly from the slope of the second regression line and the values of intercept C, which is related to the thickness of the boundary layer.

The shape of Fig. 11 confirms that the adsorption of MB onto dye-MIPs are dependent on each other, since the plot usually shows two intersecting lines depending on the exact mechanism; the first one of these lines represent surface adsorption (film diffusion) at the beginning of the interaction and the second one is the intraparticle diffusion at the end of the interaction. The plot in Fig. 11 does not pass through the origin, suggesting that intra particle diffusion is not the rate-limiting step and that some other mechanisms may also play an important role. The parameters of

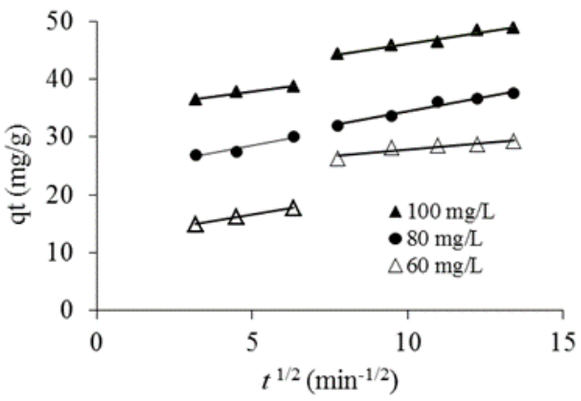

Fig. 11. Intraparticle diffusion model plot for the adsorption of MB onto dye-MIPs (volume 25 mL, dosage 0.05 g, pH 10, shaking speed 150 rpm and temp. 25°C).

Table 3
Parameter of the intra-particle diffusion model for the MB adsorption onto dye-MIPs

Concentration (mg/g)	k_{d1} (mg/g·min$^{1/2}$)	C_1	k_{d2} (mg/g·min$^{1/2}$)	C_2
60	0.901	12.061	0.456	23.291
80	1.012	23.411	0.999	24.400
100	0.716	34.311	0.822	37.892

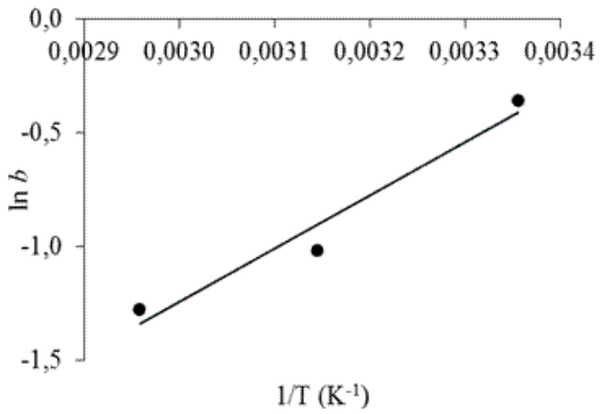

Fig. 12. Plots of ln b versus 1/T for the adsorption of MB onto dye-MIPs in aqueous solution.

intraparticle diffusion model are shown in Table 3. It can be easily observed that k_{d1} is larger than k_{d2}, indicating that film diffusion is a rapid process whereas intraparticle diffusion is a gradual process [50].

3.5. Thermodynamics adsorption

The temperature dependence performance of MB adsorption was further analyzed based on the thermodynamic parameters, such as change in free energy ΔG^o, enthalpy $\Delta H°$ and entropy $\Delta S°$. They were determined by van't Hoff equations:

$$\Delta G° = -RT \ln K_L \quad (9)$$

$$\ln b = \frac{\Delta S^o}{R} - \frac{\Delta H^o}{R \cdot T} \quad (10)$$

where R (8.314 J/mol K) is the gas constant, T (K) is the absolute temperature and b (L/mg) is the Langmuir isotherm constant. The value of enthalpy (ΔH^o) and entropy ($\Delta S°$) were calculated from the slope and intercept of the plot of ln b vs 1/T (Fig. 12). The thermodynamic parameters are shown in Table 4.

The positive values of $\Delta G°$ indicated that the adsorption of MB onto dye-MIPs was non-spontaneous. Moreover, the negative values of $\Delta H°$ indicated that the adsorption was exothermic. Therefore, the negative values of $\Delta S°$ revealed that a more ordered arrangement of MB was shaped on the surface of adsorbent [51,52]. Similar results were also obtained by Wei et al. for removal of methylene blue using $Cu_2Cl(OH)_3$ microspheres [52] and Yagub et al. for removal of methylene blue using raw pine cone powder [39].

Table 4
Thermodynamic parameters for the the MB adsorption onto dye-MIPs

Temperature (°C)	b (L/mg)	$\Delta G°$ (kJ/mol)	$\Delta H°$ (kJ/mol)	$\Delta S°$ (kJ/mol)
25	0.70	1.02	–19.35	–68.36
45	0.36	2.39		
65	0.28	3.76		

4. Conclusion

In this study, the dye-MIPs were successfully prepared using methacrylic acid (MAA) as monomers, methylene blue (MB) as a template, divinyl benzene (DVB) as a cross-linker and acetonitrile as a porogen. The obtained NIPs, as control polymer materials and dye-MIPs were used for the adsorption of MB from aqueous solutions using batch adsorption technique. The results showed that the equilibrium contact time was 60 min. The results also showed that MB adsorption onto both the NIPs and dye-MIPs was highly dependent on pH, initial concentration of MB solution and temperature. The equilibrium adsorption data of MB on both NIPs and dye-MIPs fit the Langmuir isotherm model better than Freundlich isotherm model. Based on the Langmuir isotherm model, the maximum monolayer adsorption capacity is 33.11 and 40.82 mg/g, for NIPs and dye-MIPs, respectively. In the kinetic studies, the pseudo-first-order kinetic model, pseudo-second-order kinetic model and intraparticle diffusion model were used to fit adsorption data of dye-MIPs. The pseudo-second-order kinetic model could better describe adsorption kinetics, and the intraparticle diffusion model also demonstrated the intraparticle diffusion was not the rate-limiting step. The values of thermodynamic parameters (ΔG^o, ΔH^o and ΔS^o) suggested that MB adsorption onto the dye-MIPs was an exothermic and a non-spontaneous process. This work confirms that the dye-MIP could be used for the removal of cationic dyes from wastewater.

Acknowledgements

The author is very grateful to the Institut Teknologi Bandung for the financial support of this research study through ITB Research Program 2017 No. 108f/I1.C01/PL/2017 and P3MI Research Program 2017 No.1012/I1.C01/PL/2017.

References

[1] J. Fu, Z. Chen, M. Wang, S. Liu, J. Zhang, J. Zhang, R. Han, Q. Xu, Adsorption of methylene blue by a high-efficiency adsorbent (polydopamine microspheres): Kinetics, isotherm, thermodynamics and mechanism analysis, Chem. Eng. J., 259 (2015) 53–61.

[2] Y.C. Wong, Y.S. Szeto, W.H. Cheung, G. McKay, Adsorption of acid dyes on chitosan-equilibrium isotherm analyses, Process Biochem., 39 (2004) 695–704.
[3] R.M. Mohamed, E.S. Aazam, Novel Ag/YVO4 nanoparticles prepared by a hydrothermal method for photocatalytic degradation of methylene-blue dye, J. Ind. Eng. Chem., 20 (2014) 4377–4381.
[4] M. Ghaedi, A.M. Ghaedi, F. Abdi, M. Roosta, A. Vafaei, A. Asghari, Principal component analysis-adaptive neuro-fuzzy inference system modeling and genetic algorithm optimization of adsorption of methylene blue by activated carbon derived from *Pistaciakhinjuk*, Ecotoxicol. Environ. Saf., 96 (2013) 110–117.
[5] P. Kazemi, M. Peydayesh, A. Bandegi, T. Mohammadi, O. Bakhtiari, Pertraction of methylene blue using a mixture of D2EHPA/M2EHPA and sesame oil as a liquid membrane, Chem. Pap., 67 (2013) 722–729.
[6] M. Peydayesh, A. Rahbar-Kelishami, Adsorption of methylene blue onto Platanusorientalis leaf powder: Kinetic, equilibrium and thermodynamic studies, J. Ind. Eng. Chem., 21 (2015) 1014–1019.
[7] L. Chen, A. Ramadan, L. Lv, W. Shao, F. Luo, J. Chen, Biosorption of methylene blue from aqueous solution using lawny grass modified with citric acid, J. Chem. Eng. Data, 56 (2011) 3392–3399.
[8] Y. Li, Q. Du, T. Liu, X. Peng, J. Wanga, J. Sun, Y. Wang, S. Wu, Z. Wang, Y. Xia, L. Xia, Comparative study of methylene blue dye adsorption onto activated carbon, graphene oxide, and carbon nanotubes, Chem. Eng. Res. Des., 91 (2013) 361–368.
[9] C. Li, H. Zhong, S. Wang, J. Xue, Z. Zhang, Removal of basic dye (methylene blue) from aqueous solution using zeolite synthesized from electrolytic manganese residue, J. Ind. Eng. Chem., 23 (2015) 344–352.
[10] Y. Liu Y. Zheng, A. Wang, Enhanced adsorption of Methylene Blue from aqueous solution by chitosan-g-poly (acrylic acid)/vermiculite hydrogel composites, J. Environ. Sci., 22 (2010) 486–493.
[11] R. Sanghi, B. Bhattacharya, Review on decolorisation of aqueous dye solutions by low cost adsorbents, Color Technol., 18 (2006) 256–269.
[12] D. Shen, J. Fan, W. Zhou, B. Gao, Q. Yue, Q. Kang, Adsorption kinetics and isotherm of anionic dyes onto organo-bentonite from single and multisolute systems, J. Hazard. Mater., 172 (2009) 99–107.
[13] S. Dawood, T.K. Sen, Review on dye removal from its aqueous solution into alternative cost effective and non-conventional adsorbents, J. Chem. Proc. Eng., 1 (2014) 1–7.
[14] I.A. Oke, N.O. Olarinoye, S.R.A. Adewusi, Adsorption kinetics for arsenic removal from aqueous solutions by untreated powdered eggshell, Adsorption, 14 (2008) 73–83.
[15] H. Hashemi-Moghaddam, F. Yahyazadeh, Synthesis a new adsorbent of molecularly imprinted polymer for absorb the silver ions from biological sample, E3S Web of Conferences, 1 (2013) 39001–39004.
[16] G.Z. Kyzas, D.M. Bikiaris, Molecular imprinting for high-added value metals: an overview of recent environmental applications, Adv. Mater. Sci. Eng., 2014 (2014) 1–8 Article ID 932637.
[17] Z. Terzopoulou, M. Papageorgiou, G.Z. Kyzas, D.N. Bikiaris, D.A. Lambropoulou, Preparation of molecularly imprinted solid-phase microextraction fiber for the selective removal and extraction of the antiviral drug abacavir in environmental and biological matrices, Anal. Chim. Acta, 913 (2016) 63–75.
[18] Y.A. Olcer, M. Demirkurt, M.M. Demir, A.E. Eroglu, Development of molecularly imprinted polymers (MIPs) as a solid phase extraction (SPE) sorbent for the determination of ibuprofen in water, RSC Adv., 7 (2017) 31441–31447.
[19] H.S. Byun, Y.N. Youn, Y.H. Yun, S.D. Yoon, Selective separation of aspirin using molecularly imprinted polymers, Sep. Purif. Technol., 74 (2010) 144–153.
[20] H. Liu, X. Lei, Y. Zhai, L. Li, Electrospun nanofiber membranes containing molecularly imprinted polymer (MIP) for Rhodamine B (RhB), Adv. Chem. Eng. Sci., 2 (2012) 266–274.
[21] Y. Liu, M. Meng, J. Yao, Z. Da, Y. Feng, Y. Yan, C. Li, Selective separation of phenol from salicylic acid effluent over molecularly imprinted polystyrene nanospheres composite alumina membranes, Chem. Eng. J., 286 (2016) 622–631.
[22] Y. Zhang, J. Zhang, Q. Liu, Gas sensors based on molecular imprinting technology, Sensors, 17 (2017) 1567–1581.
[23] G. Selvolini, G. Marrazza, MIP-based sensors: Promising new tools for cancer biomarker determination, Sensors, 17 (2017) 718–737.
[24] P. Dzygiel, E. O'Donnell, D. Fraier, C. Chassaing, P.A.G. Cormack, Evaluation of water-compatible molecularly imprinted polymers as solid-phase extraction sorbents for the selective extraction of sildenafil and its desmethyl metabolite from plasma samples, J. Chromatogr. B, 853 (2007) 346–353.
[25] N.M. Bergmann, N.A. Peppas, Molecularly imprinted polymers with specific recognition for macromolecules and proteins, Prog. Polym. Sci., 33 (2008) 271–288.
[26] M. Le Noir, A.S. Lepeuple, B. Guieysse, B. Mattiasson, Selective removal of 17 [beta]-estradiol at trace concentration using a molecularly imprinted polymer, Water Res., 41 (2007) 2825–2831.
[27] Y. Li, X. Li, J. Chu, C. Dong, Synthesis of core-shell magnetic molecular imprinted polymer by the surface RAFT polymerization for the fast and selective removal of endocrine disrupting chemicals from aqueous solutions, Environ. Pollut., 158 (2010) 2317–2323.
[28] M.A. Zulfikar D. Wahyuningrum, R.R. Mukti, H. Setiyanto, Molecularly imprinted polymers (MIPs): a functional material for removal of humic acid from peat water, Desal. Water Treat., 57 (2016) 15164–15175.
[29] E.V. Piletska, A.R. Guerreiro, M. Romero-Guerra, I. Chianella, A.P.F. Turner, S.A. Piletsky, Design of molecular imprinted polymers compatible with aqueous environment, Anal. Chim. Acta, 607 (2008) 54–60.
[30] S. Asman, N.A. Yusof, A.H. Abdullah, M.J. Haron, Synthesis and characterization of a molecularly imprinted polymer for methylene blue, Asian J. Chem., 23 (2011) 4786–4794.
[31] S. Asman, N.A. Yusof, A.H. Abdullah, M.J. Haron, Synthesis and characterization of hybrid molecularly imprinted polymer (MIP) membranes for removal of methylene blue (MB), Molecules, 17 (2012) 1916–1928.
[32] N. Wang, S.J. Xiao, C.W. Su, Preparation of molecularly imprinted polymer for methylene blue and study on its molecular recognition mechanism, Colloid Polym. Sci., 294 (2016) 1305–1314.
[33] G.Z. Kyzas, D.N. Bikiaris, N.K. Lazaridis, Selective separation of basic and reactive dyes by molecularly imprinted polymers (MIPs), Chem. Eng. J., 149 (2009) 263–272.
[34] T. Madrakian, A. Afkhami, M. Ahmadi, H. Bagheri, Removal of some cationic dyes from aqueous solutions using magnetic-modified multi-walled carbon nanotubes, J. Hazard. Mater., 196 (2011) 109–114.
[35] B.K. Nandi, A. Goswami, M.K. Purkait, Adsorption characteristics of brilliant green dye on kaolin, J. Hazard. Mater., 161 (2009) 387–395.
[36] M. Ghaedi, A.G. Nasab, S. Khodadoust, M. Rajabi, S. Azizian, Application of activated carbon as adsorbents for efficient removal of methylene blue: Kinetics and equilibrium study, J. Ind. Eng. Chem., 20 (2014) 2317–2324.
[37] R. Ahmad, R. Kumar, Conducting polyaniline/iron oxide composite: a novel adsorbent for the removal of amido black 10B, J. Chem. Eng. Data, 55 (2010) 3489–3493.
[38] H. Hou, R. Zhou, P. Wu, L. Wu, Removal of Congo red dye from aqueous solution with hydroxyapatite/chitosan composite, Chem. Eng. J., 211–212 (2012) 336–342.
[39] M.T. Yagub, T.K. Sen, M. Ang, Removal of cationic dye methylene blue (MB) from aqueous solution by ground raw and base modified pine cone powder, Environ. Earth Sci., 71 (2014) 1507–1519.
[40] Z. Shahryari, A.S. Goharrizi, M. Azadi, Experimental study of methylene blue adsorption from aqueous solutions onto carbon nano tubes, Int. J. Water. Resour. Environ. Eng., 2 (2010) 16–28.

[41] M. Dogan, H. Abak, M. Alkan, Adsorption of methylene blue onto hazelnut shell: kinetics, mechanisms and activation parameters., J. Hazard. Mater., 164 (2009) 172–181.
[42] Y. Özdemir, M. Dog˘an, M. Alkan, Adsorption of cationic dyes from aqueous solutions by sepiolite, Microporous Mesoporous Mater., 96 (2006) 419–427.
[43] K.W. Jung, B.H. Choi, M.J. Hwang, T.U. Jeong, K.H. Ahn, Fabrication of granular activated carbons derived from spent coffee grounds by entrapment in calcium alginate beads for adsorption of acid orange 7 and methylene blue, Bioresour. Technol., 219 (2016) 185–195.
[44] Y. Feng, H. Zhou, G. Liu, J. Qiao, J. Wang, H. Lu, L. Yang, Y. Wu, Methylene blue adsorption onto swede rape straw (Brassica napus L.) modified by tartaric acid: Equilibrium, kinetic and adsorption mechanisms, Bioresour. Technol., 125 (2012) 138–144.
[45] J. Yu, R. Chi, Y. Zhang, Z. Xu, C. Xiao, J. Guo, A situ co-precipitation method to prepare magnetic PMDA modified sugarcane bagasse and its application for competitive adsorption of methylene blue and basic magenta, Bioresour. Technol., 110 (2012) 160–166.
[46] K. Khaled, A. El-Nemr, A. El-Sikaily, O. Abdelwahab, Removal of Direct N Blue 106 from artificial textile dye effluent using activated carbon from orange peel: Adsorption isotherm and kinetic studies, J. Hazard. Mater., 165 (2009) 100–110.
[47] G. McKay, The adsorption of dyestuff from aqueous solution using activated carbon: analytical solution for batch adsorption based on external mass transfer and pore diffusion, Chem. Eng. J., 27 (1983) 187–195.
[48] M.F. Elkady, A.M. Ibrahim, M.M. Abd El-Latif, Assessment of the adsorption kinetics, equilibrium and thermodynamic for the potential removal of reactive red dye using eggshell biocomposite beads, Desalination, 278 (2011) 412–423.
[49] M.A. Zulfikar, H. Setiyanto, Rusnadi, L. Solakhudin, Rubber Seeds (*Heveabrasiliensis*): An adsorbent for adsorption of Congo Red from aqueous solution, Desal. Water Treat., 56 (2015) 2976–2987.
[50] Z. Chen, J. Zhang, J. Fu, M. Wang, X. Wang, R. Han, Q. Xu, Adsorption of methylene blue onto poly(cyclotriphosphazene-co-4,4′-sulfonyldiphenol) nanotubes: Kinetics, isotherm and thermodynamics analysis, J. Hazard. Mater., 273 (2014) 263–271.
[51] Z.J. Wu, H. Joo, K. Lee, Kinetics and thermodynamics of the organic dye adsorption on the mesoporous hybrid xerogel, Chem. Eng. J., 112 (2005) 227–236.
[52] W. Wei, P. Gao, J. Xie, S. Zong, H. Cui, X. Yue, Uniform $Cu_2Cl(OH)_3$ hierarchical microspheres: A novel adsorbent for methylene blue adsorptive removal from aqueous solution, J. Solid State Chem., 204 (2013) 305–313.